Incremental Interface Surface Potential Measured with a Nano-Gap Coplanar Device Structure and Its Applications

H.-T. Hsueh[a], P.-H. Chen[b], F.-E. Chen[c], M.S. Tsai[b], T.-W. Wu[b] and C.-T. Lin[a,b,c]

[a] Graduate Institute of Biomedical Electronics and Bioinformatics, National Taiwan University, Taipei, 106, Taiwan
[b] Graduate Institute of Electronics Engineering, National Taiwan University, Taipei 106, Taiwan
[c] Department of Electrical Engineering, National Taiwan University, Taipei 106, Taiwan

In traditional capacitive-based biomolecular sensing technologies, it is important to have an uniform and defect-free interface layers. However, efforts to achieve the interface layer are tedious and labor intensive. To enhance the sensing characteristics of capacitive-based biomolecular sensing device, we use co-planar electrode with nano-gap structure. Different from traditional capacitive sensing devices, the biomolecular sensing elements are placed on the gap surface rather than on the electrode surface. This arrangement leads to gap-surface charge changes as molecular binding. And the altered gap-surface charges change the electrical double layer (EDL) capacitance of the sidewall of nano-gap electrodes. This results in the change of the nano-gap capacitance. Based on this idea, we demonstrates a cTnT detection with detection range of 100 pg/ml to 10 μg/ml. In addition, we also show both gap width and detection environment play important roles in sensitivity and detection limit of the proposed nano-gap biosensing devices.

Introduction

Capacitive biosensor is one kind of impedance biosensor based on impedimetric transduction and owns its great attractions due to their simple structure to perform label-free detection. These devices provide effective methods for monitoring analytes with many advantages over other techniques, such as low cost, fast response and mass-production capability. Moreover, in contrast with other electrochemical sensors, no reference electrode required simplifies measurement setup and permits sensor further miniaturized. In the recent years, a wide range of different capacitive biosensors was reported to detect variety analysts. Capacitive biosensors is used to register changes of charges at the electrodes surface modified by insulation layer and bio-recognition element. In order to perform ideal capacitor, non-faradaic process is necessary to accumulate charges. Hence, the quality of insulation layer is the most critical issue in capacitive biosensor. To overcome the problems, we have proposed using co-planar electrodes with nanometer gap and placing bio-recognition element between electrodes for cTnT detection. It is well known surface potential generates electric double layer (EDL) in buffer solution. As charged analytes binding on the gap surface, tuning the gap surface charges and modulating gap surface ion distribution, the thickness of electric

double layer or Debye length from electrodes sidewall changes. This change induces the difference in electric double layer capacitance (EDLC) measurement. Hence, this capacitance measurement provides a novel solution to overcome the insulator issues on the electrode.

In capacitive sensing, one perfect insulation layer is necessary to form ideal capacitor on the electrode surface. The bio-recognition element will further immobilized on the insulation layer surface to form another capacitive layer. The insulation layer capacitor (Ci) and the bio-recognition capacitor (Cb) are connected in series between the electrode and buffer solution. To make sure the Cb difference can dominate the total capacitance difference, it is essential to increase Ci/Cb ratio. The capacitance is based on the basic equation : $C = \varepsilon_0 \varepsilon_r * A/d$, where ε_0 and ε_r represent vacuum permittivity and relative permittivity of dielectric material, respectively, and where d and A represent capacitor distance and area, respectively. Thinner insulation layer through deposition or forming self-assembly layer through immobilization both provides possible solution. However, thinner insulator also induces one lethal problem, that is, the increment of defect possibility. The defect increases the leakage current which bypasses the insulation layer and gives the decrement for capacitance. As a consequence, the insulator thickness and defect possibility are trade-off variables. This uncertainty restrict the detection limit and sensitivity of traditional capacitance sensor.

To address above issue in capacitive sensing, putting bio-recognition element between electrodes in our report provides one alternative solution to overcome this trade-off situation. The immobilized bio-recognition element between electrodes not merely alters the detection location but also change the sensing current path from bulk solutions to near-surface regions. Traditional capacitive sensing mechanism forms two capacitive layers on the electrode surface by insulate material and bio-recognition element. And the sensing mechanism relies on the capacitive change of bio-recognition elements. In our device, in contrast, the bio-recognition elements are on the gap surface. As bio-recognition elements changes, the gap surface potential is changed because of the different net charge distribution on the surface. And the gap surface potential modulates the electrode side-wall capacitance, i.e. the electric double layer capacitance (EDLC). The electric behavior of EDL can be equivalent to a capacitor across the interface. Hence, through capacitance measurement, the gap surface potential modulated by bio-recognition element can be detected. In the proposed mechanism, it is not necessary to generate one perfect insulation layer on the electrode surface. As a consequence, the detection property could further improve by overcoming the trade-off situation.

To measure the EDLC difference induced by the gap surface potential in this work, we proposed simple nano-gap structure with coplanar electrode device for measurements of incremental capacitance changes. According to Gouy-Chapman theory of double electric layer model, the thickness of EDLC, also called Debye length, is only about few nanometer to tens of nanometer depending on electrolyte concentration. That is, the gap surface potential can only affect the ion distribution about tens of nanometer from the surface. That is the reason why the traditional capacitor sensor above micrometer-scale is difficult to observe the gap surface impact. Hence, coplanar electrode and nano-gap structure are both necessary condition to concentrate the electrolyte current near the gap surface for EDLC measurement. And then, we use electrochemistry impedance spectroscopy (EIS) and cyclic voltammetry (CV) to measure the capacitance difference. Utilizing EIS method with different modified functional group for capacitance measurement demonstrates the relationship between of surface potential and measured capacitance. We further proposed two-pathway model and verify the proposed model by

using the explanation of electrode side wall debye length contraction phenomenon. To further demonstrate an application of the proposed sensing device, we further used cTnT antigen-antibody pair, a major biomarker of myocardial necrosis, to show the biosensor application based on our proposed method.

Materials and Methods

Sensor Design and Fabrication

The fabrication of nano-gap device started from one 4 inches silicon wafer with a 300 nm thermally grown silicon dioxide on the surface. After cleaning the wafer by acetone and isopropyl alcohol, E-beam lithography (Elionix ELS-7000) was used to define 100nm, 200nm and 1μm nano-gap pattern. Then, the surface thermal oxide was etched back 25 nm by reactive ion etch (RIE). The followings is using E-gun to deposit 5 nm Cr and 45 nm Au before removing E-beam photoresist. Finally, using 10% NaOH solution to lift off and form coplanar electrodes. It must be emphasized that only Au-electrode surface was exposed to surrounded environments based on this fabrication process as shown in Fig.1. The height between the top surface of Au electrode and the nano-gap oxide surface was 25 nm, which corresponds to the length of the antibody used in following experiments.

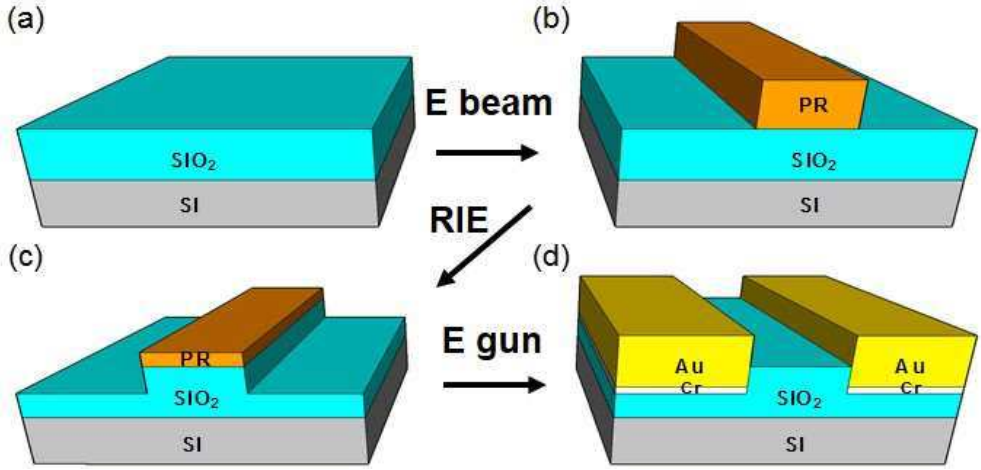

Figure 1. Schematic of fabrication flow

Surface Functionalization and Antibody Immobilization

To have surface functional group replacement experiment and biomolecular sensing experiments, the fabricated coplanar electrodes devices were cleaned by $NH_4OH/H_2O_2/H_2O$ (in 1:1:5 weight ratio, respectively) for 20 minutes at 70 ℃ to remove organic residues. After deionized water treatment, the cleaned devices were immersed in 2% (v/v) aminopropyldimethylmethoxysilane (APDMMS) in ethanol for 12 hours at room temperature to form monolayer on the surface and expose amine group facing to the surface. APDMMS forms more uniform and denser monolayer than 3-aminopropyltriethoxysilane (APTES) does which is common used in biosensor. The ethanol residues was removed by 120 ℃ baking for 20 minutes. At this stage, the amino termination gives positively charged surface in PBS buffer solutions. After measurements, the devices were soaked in 2.5% glutaraldehyde solution for 1 hour at room temperature to form next monolayer through covalent bonding. Glutaraldehyde treatment transfers surface functional group from amino group to aldehyde group. It is well-known the aldehyde group is near neutral in the PBS buffer solution, total surface charges decrease

in this procedure. To make surface negatively charged for further investigate, 10 μg/ml 3-aminobenzoic acid is injected for 1 hour to transfer the aldehyde group to carboxyl group, which is negatively charged at pH 7. For bio-functional examination of the implemented coplanar electrode devices, injecting 1 mM 1-Ethyl-3-(3-dimethylaminopropyl)carbodiimide/N-Hydroxysuccinimide (EDC/NHS) solution to activate the carboxyl group from the previous experiment for 20 minutes and form amide bond with the amine group of antibody through condensing reaction. After washing out EDC/NHS, 10 μg/ml cTnT antibody is added and incubated for overnight at 4℃ for immobilization on the surface. Then the device was ready for the cTnT sensing experiment.

Impedance Measurement Methods

An electrochemical impedance spectroscopy (EIS) was also performed by SP-150 potentiostat (BioLOGIC Inc.) with low current module which has a current resolution around 76 femto ampere and EC-Lab® software package. In this work, EIS measurements were set in a frequency ranging from 0.1 Hz-10 kHz and a sinusoidal amplitude of 10 mV to measure the impedance and capacitance of the electric double layer between the nano-gap devices. These EIS experimental results were measured in a Faraday cage to prohibit EMI. We defined capacitance variance ratio $R(\%) = (C' - C_0)/C_0$, where C_0 and C' represents the capacitance before and after treatment respectively at the 0Hz which capacitance is EDLC in the experiment setup.

Cyclic voltammetry (CV) was used to measure the differential capacitance of the nano gap between the two coplanar electrodes. This electrochemical property was characterized by a device parameter analyzer (Agilent B1500A). The voltage operation range was from -0.1V to 0.1V. The scan rate was 400 mV/min and step voltage was 2 mV. All the measurement was also performed in a Faraday cage to prohibit EMI. We defined capacitance variance ratio $R(\%) = (C' - C_0)/C_0$, where C_0 and C' represents the capacitance before and after treatment respectively. The capacitance is equal to average current divided by scan rate.

Results and Discussions

Impedance Measurement Methods

To make sure the surface potential on the silicon dioxide surface will influent the CV curve, we immobilized different crosslinkers carried different function groups. At first, the silicon dioxide surface was derivatives with APDMMS and then 2.5% glutaraldehyde immobilized on the resulting APDMMS. Figure 2(a) show the CV result during the glutaraldehyde immobilized process. Because the aldehyde group from glutaraldehyde bring less charge than amine group from APDMMS under PBS buffer solution. Moreover, previous functional group will form covalent bond with next monolayer, hence the previous functional group show tiny effect on the surface potential. When the glutaraldehyde immobilize on the APDMMS, the surface charge will decrease gradually during reaction. Figure 2(b) provides the correlation between the capacitor shift and reaction time. The X-axis represent the capacitor variance ratio compared to the APDMMS result at zero voltage where the minimum redox reaction probability under symmetric electrode device has. It can be seen from the result above, the capacitor decrease dramatically in the beginning and, after sixty minutes, the capacitor become stable because of the equilibrium of aldehyde amine condensing reaction. Once the glutaraldehyde was immobilized, 3-aminobenzoic acid was further injected in it. Because

the aldehyde group from glutaraldehyde will also react with the amine group from 3-aminobenzoic acid, the 3-aminobenzoic acid can immobilized on the glutaraldehyde surface and exposed the carboxyl group to the surface. Figure 2(c) show the experimental data on the 3-aminobenzoic acid immobilization. As result of higher electronegativity on carboxyl group than on aldehyde group, carboxyl group carry more charges than aldehyde group does. Total charge between the electrode increases gradually during immobilization process and causing the capacitor raise (Figure 2(d)). There was a significant positivity correlation between the polarities from surface functional group and measured capacitor. Moreover, interestingly, amine group and carboxyl both increase the capacitor. The fact indicates that the charge quantity will affect capacitor but charge type won't. Furthermore, we also applied our devices under oxygen plasma treatment to charge the silicon dioxide. The result also indicated the surface potential increment would increase the capacitor. Because the electric characteristic of gold electrode does not change during oxygen plasma treatment, but the silicon dioxide surface would full of negative charge form oxygen ion. Hence, the capacitor increment would only cause from the negative charge on the silicon dioxide surface. Moreover, the capacitor was increase more apparently under higher power oxygen plasma treatment. It is because higher power would penetrated more oxygen ion into the silicon dioxide so that the silicon dioxide could carry more negative charge. The above experimental results tell the truth that the surface potential variation form silicon dioxide can be measured as long as the electrode retain persistence. The results also coordinate with the measurement model we proposed.

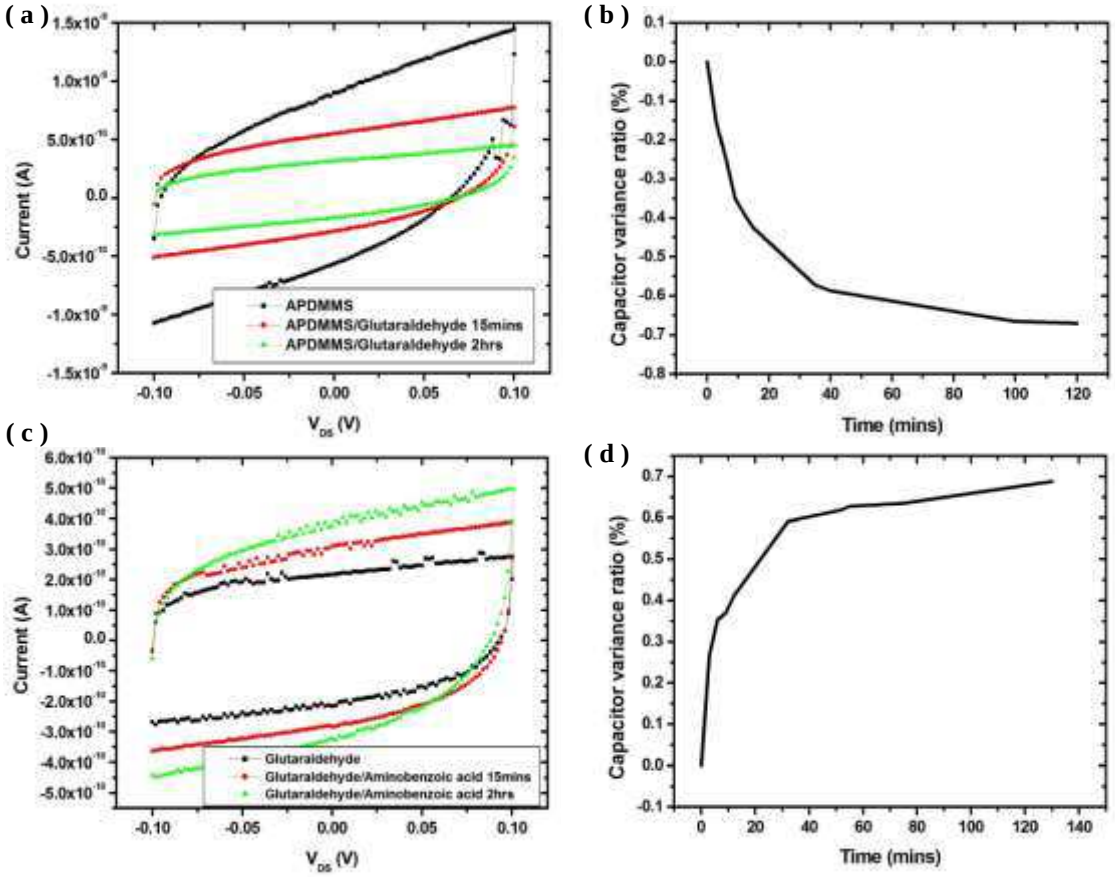

Figure 2. The CV curves and capacitor variance ratio under different functional group modification. (a) The CV curves response as the glutaraldehyde immobilizing on the APDMMS monolayer surface. (b) The temporal response of the capacitor variation ratio during glutaraldehyde immobilization process. (c) The CV curves response as the 3-

aminobenzoic acid immobilizing on the glutaraldehyde monolayer surface. (d) The temporal response of the capacitor variation ratio during 3-aminobenzoic acid immobilization process.

Then the device was treated with cTnT antibody and prepared for cTnT antigen detection. In order to check the selectivity and non-specific binding, 10 μ g/ml BSA was introduced after the PBS buffer solution for blank test. Until the capacitor became stable, and the result didn't shift anymore, 1 μ g/ml cTnT antigen was introduced for specific binding. As shown in Figure 3a, the observed capacitor show slightly different after three minutes. Even until the capacitor become stable, the capacitor only decrease about 8%. As a result of no apparent shift at three minutes, the following results are measured after three minutes. However, After the 1 μ g/ml cTnT injecting for three minutes, the capacitor decrease 22% (Figure 3a). The result strongly prove our device has high selectivity and the non-specific binding has little influence on the observed capacitor. Thus, for sensitivity test, we mixed 10 μ g/ml BSA with different concentration of cTnT antigen. Figure 3b and 3c presents the experimental data and capacitor variance on sensitivity result in respectively. The dynamic range of the cTnT antigen is from 100pg/ml to 1 μ g/ml. The blank test also prove the selectivity again in Figure 3c. Moreover, it should be noted that we measured the charge variance on the gap surface and Figure 2 also demonstrates the capacitor increment from the surface charge. However, it seems that Figure 4 show the reverse result when there are more charged cTnT antigen binding on the gap surface. The most possible explanation is that the cTnT antibody and antigen carry the opposite charge. As the antigen recognized by the antibody, local charged would be compensated and neutralized. Hence, the total charge on the surface would decrease. To verify the assumption, we used 2D electrophoresis to check the pI value of the antigen and antibody. The 2D electrophoresis result point out the pI value of cTnT antigen is less than 6 and the antibody light chain is about 8. Thus, the antigen is negative and antibody is positive in the PBS buffer (pH=7.2). As the antigen binding on the antigen, the total surface charge and measured capacitor will decrease.

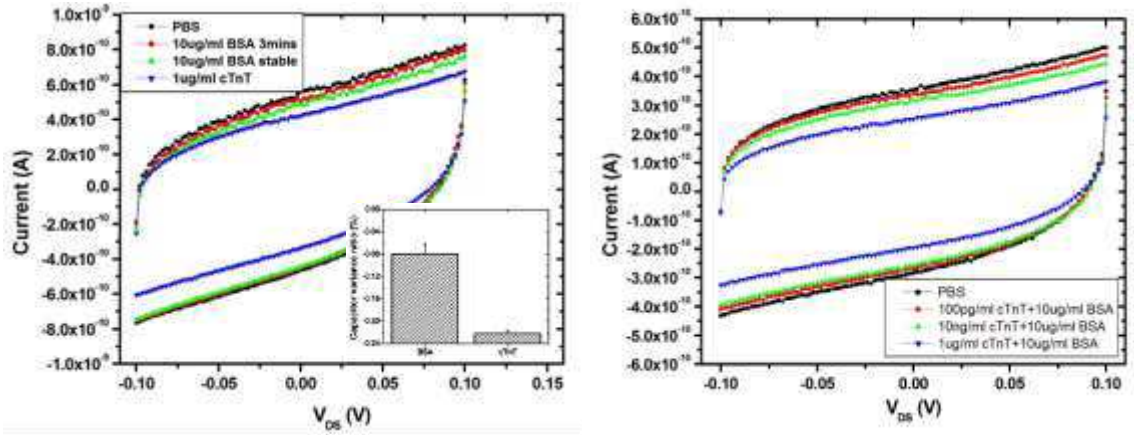

Figure 3. (a) The selectivity result measured by cyclic voltammetry and the black, red, green, blue curves represent the serial response of the initial state, 10ug/ml BSA injected for 3mins, 10ug/ml BSA injected until stable and 1ug/ml cTnT injected, respectively. The inset represent the capacitor variance ratio compares to the nonspecific binding(BSA) and specific binding(cTnT). (b) The sensitivity result measured by cyclic voltammetry at different cTnT concentration with 10ug/ml BSA as background. The black, red, green,

blue curves represent the serial response of the initial state, 100pg/ml cTnT, 10ng/ml cTnT and 1ug/ml cTnT, respectively.

Conclusions

In the previous serial experiments, we have demonstrated one novel surface potential variation measurement method by decreasing the dimension of the gap between two electrodes to nano-scale. Immobilizing different surface functional group proves the capacitor variation correlated to the quantity of surface charge. This feature provide some applications for biomarker detection by measuring capacitor different causing form charged antigen through specific binding. The dynamic range for cTnT detection is from 100pg/ml to 10 μ g/ml in 0.01XPBS buffer solution. Moreover, we also show the buffer concentration influents the limit of detection for cTnT examination. 0.01X PBS buffer condition provide lower LOD than 1XPB buffer. Thus, the nano-gap devices provide a simple but powerful and reliable platform for surface potential variance detection and can be used for multiple chemical and clinical examination.

Acknowledgments

The authors would like to thank the financial supporting from Ministry of Science and Technology (MOST) in Taiwan (104-2221-E-002-164-MY2 and 104-2628-E-002-014-MY3) and National Taiwan University (104R890943).

References

1. Apple, F.S., Wu, A.H., Mair, J., Ravkilde, J., Panteghini, M., Tate, J., Jaffe A.S., 2005. Clinical Chemistry 51, 810-824.
2. Carrara, S., Benini, L., Bhalla, V., Stagni, C., Ferretti, A., Cavallini, A., Samorì, B., 2009. Biosensors and Bioelectronics, 24, 3425-3429.
3. Hatsuki, R., Yujiro, F., Yamamoto, T., 2013. Microfluidics and nanofluidics, 14, 983-988.
4. Hsueh, H.-T. and Lin, C.-T., 2016, Biosensors and Bioelectronics, 79, 2016, 636-643.
5. Itoh, Y., Kim, B., Gearba, R. I., Tremblay, N.J., Pindak, Matsuo, R., Nakamura, Y.E., Nuckolls, C., 2011. Chem. Mater, 23, 970-975.
6. Kallempudi, S.S., Gurbuz, Y., 2011. Sensors and Actuators B: Chemical, 160, 891-898.
7. Li, H., Bashir, R., 2002. Sensors and Actuators B: Chemical, 86, 215-221.
8. Qureshi, A., Niazi, J. H., Kallempudi, S., Gurbuz, Y., 2010. Biosensors and Bioelectronics, 25, 2318-2323.
9. Santos, A., Davis, J.J., Bueno, P.R., 2014. J Anal Bioanal Tech S, 7, 2.
10. Wang, H., Pilon, L., 2012. Electrochimica Acta, 76, 529-531.
11. Yuan, H., Shimotani, H., Ye, J., Yoon, S., Aliah, H., Tsukazaki, A., Iwasa, Y., 2010. Journal of the American Chemical Society, 132, 18402-18407.